

Parametric Phase Tracking

via Expectation Propagation

Leszek Szczecinski and Hsan Bouazizi

Abstract

In this work we propose a simple algorithm for signal detection in a single-carrier transmission corrupted by a strong phase noise. The proposed phase tracking algorithm is formulated within the framework of parametric message passing (MP) which reduces the complexity of the Bayesian inference by using distributions from a predefined family; here, of Tikhonov distributions. This stays in line with previous works mainly inspired by the well-known Colavolpe–Barbieri–Caire (CBC) algorithm which gained popularity due to its simplicity and possibility for decoder-aided operation. In our work we leverage the simplicity of the MP characteristic of the CBC algorithm and combine it with the principles of the expectation propagation (EP). In this way we notably improve the performance of the phase tracking before the decoder’s feedback can be even considered. Further, in the spirit of the joint decoding and phase tracking, the EP algorithm can be integrated in the decoding loop; then, not only it outperform the reference scenario of the exact (discretized) message passing – a results that was not yet shown in the literature, but it requires much lower complexity than the state-of-the art algorithms.

Index Terms

expectation propagation, circular moment matching, phase noise, phase tracking, Tikhonov distributions

I. INTRODUCTION

In this work we propose a simple algorithms for signal detection in transmission corrupted by a phase noise. The proposed parametric solution is shown to outperform the state-of-the-art parametric algorithms both in terms of attainable error rates and of the complexity.

L. Szczecinski is with INRS-EMT, University of Quebec, Montreal, Canada. e-mail: leszek@emt.inrs.ca

H. Bouazizi was with INRS-EMT, University of Quebec, Montreal, Canada. e-mail: bouazizi@emt.inrs.ca

We consider here the single-carrier transmission which is often used for high speed communication in frequency non-selective medium e.g., in satellite channels [1], wireless backhaul [2] or optical communications [3] [4]. The limiting factor in achieving a high spectral efficiency is then not only the additive white Gaussian noise (AWGN) but also the phase-noise which is caused by the instability of the phase reference (such as a laser or an RF oscillator).

Although sometimes the concept of “strong” phase noise is used, it merely depends on the constellation size: with sufficiently large modulation, the phase noise becomes a limiting factor for reliable communications. It is especially true for the wireless backhaul and optical channel which aggressively increase the modulation size [2] [3] [4]. The wireless backhaul, for example, calls for the use of constellation which may contain thousands of points [2].

Since the phase noise is a random process with memory, the term “phase tracking” is often used and the common strategy relies on pilots symbols which, providing reliable reference, facilitate the tracking of the phase for payload symbols. Increasing the density of the pilots, usually improves the performance at the cost of decreased spectral efficiency. Therefore, the challenge of the phase tracking is not to eliminate the pilots altogether but rather to attain desirable performance (as measured by the errors rates) with the limited number of pilots.

The problem of phase tracking can be solved optimally (in the probabilistic sense) via the message passing (MP) defined over the graph relating all the involved variables [1]. It allows us to track the distribution of the phase at each symbol but, to represent accurately the distributions, a large number of samples may be required [1] [5] even if simplifications may be sought by truncating the support of the distributions [2].

Therefore, many works looked into the possibility of *parametric* phase tracking, where the distributions of the phase is assumed to belong to a predefined family; Tikhonov distributions [1] [5] or Gaussians [6] [4] are the most popular choices. Then, instead of estimating the distribution, only a few parameters need to be tracked.

The distributions in the MP are naturally mixtures (result of averaging the contribution of the unknown payload symbols over the entire constellation), with potentially large number of elements. The mixture reduction is thus at the heart of any parametric phase tracking, and consists in replacing the mixture with a member from the adopted family of distributions. The way in which the mixture reduction is done, affects the implementation complexity and performance. Thus, the art of parametric MP resides in finding a right balance between these two, often,

contradictory criteria.

With that regard, the Colavolpe–Barbieri–Caire (CBC) algorithm [1] makes uttermost simplification of the mixtures that produces a very simple MP; due to its simplicity it should be considered “canonical” in that context. However, the cost is paid with relatively poor performance which must be improved by leveraging the presence of the decoder as only in this way the CBC algorithm can exploit the information about the modulation constellation. The resulting joint phase tracking and decoding relies on the iterative exchange of information between the phase tracking and the decoder. This approach has been often reused, e.g., [7] [4].

It is not without the pitfalls, however, and it was shown in [6] that, for large coding rates the CBC algorithm introduces an error floor. The remedy is then sought in [5] [6] by exploiting explicitly the form of the constellation and changing the way the mixture reduction is performed: the performance is improved but the resulting MP is also more complex.

What the CBC algorithm and many previous works on the parametric MP have in common is to rely heavily on the decoder to improve the estimation of the phase via joint decoding - phase tracking. The notable difference is [5] which mimics the behaviour of the discretized message passing (DMP). However, the improvement is attained by making the parametrization much more involved both in terms of the number of required parameters and their estimation.

In that regard, our take on this problem is different: we want to i) leverage the simplicity inherent in the MP of the CBC algorithm, and ii) exploit the structure of the constellation *without* relying *only* on the decoder’s feedback; in fact, this is what the DMP actually does and yet its performance is often taken as the reference for the phase tracking algorithm which *do use* the decoder’s feedback.

We propose to apply the expectation propagation (EP) [8] which is a general framework for iterative refinement of the approximations in parametric MPs. The EP phase tracking algorithm we derive, preserves the simplicity characteristic of the MP of the CBC algorithm, is thus simpler than the alternative proposed in [6], and yet outperforms the DMP, which is often treated as a performance limit for the phase tracking algorithms.

The rest of the paper is organized as follows. In Sec. II, we introduce the adopted system model, in Sec. III we outline the fundamentals of the Bayesian phase tracking while its parametric formulation is explained in Sec. IV, where we also show how the the “canonical” algorithm from [1] may be significantly improved by considering explicitly the circular nature of the involved

distributions.

The main contribution lies in Sec. V which explains how the EP framework may be used to derive a new phase tracking algorithm which, as shown in numerical examples, improves the performance without any help from the decoder. We also show that, when combined with the decoder, the new algorithms surpasses the DMP limits conventionally used to evaluate the phase tracking algorithms. The conclusions are drawn in Sec. VI and the appendices show the details of the operations on the circular distributions, clarifying the analytical details and providing new approximations.

II. SYSTEM MODEL

We consider transmission over a channel corrupted by the additive noise and phased noise

$$y_n = x_n e^{j\theta_n} + v_n, \quad n = 0, \dots, N \quad (1)$$

where x_n is the transmitted complex symbol, y_n are samples of the received signal, v_n is the additive noise, and θ_n is the phase noise. We model v_n as AWGN, i.e., a complex independent, identically distributed (i.i.d.) Gaussian variables with zero mean and variance N_0 ; θ_n is modelled as a Wiener process

$$\theta_n = \theta_{n-1} + w_n, \quad n = 1, \dots, N, \quad (2)$$

where w_n are i.i.d. zero-mean, real Gaussian variables with variance σ_w^2 ; the initial values θ_0 are modelled as uniformly distributed over the interval $(-\pi, \pi]$.

This model is popular in wireless and optical communications, e.g., [1] [4]. The variance of the additive noise v_n is determined by the thermal/optical noise at the receiver and the attenuation on the propagation path; the signal-to-noise ratio (SNR) is defined as $\text{snr} = \frac{1}{N_0}$. The variance of the phase noise w_n reflects the (in)stability of the oscillator used in the demodulation process. We suppose that both, σ_w^2 and snr , are known at the receiver.

The transmitted symbols x_n are obtained via bit-interleaved coded modulation (BICM) [9, Chap. 1.4]. That is, i) the information bits $\mathbf{b} = [b_1, \dots, b_{N_b}]$ are encoded using the binary encoder of rate r into the sequence of coded bits $\mathbf{c} = [c_1, \dots, c_{N_c}]$, where $N_b = rN_c$; in the numerical examples we use the low-density parity-check (LDPC) codes, ii) the coded bits \mathbf{c} are

regrouped into length- m labels $\tilde{\mathbf{c}}_n = [c_{n,1}, \dots, c_{n,m}]$, i.e., $\mathbf{c} = [\tilde{\mathbf{c}}_1, \dots, \tilde{\mathbf{c}}_{N_s}]$ which are mapped onto the symbols from the \mathcal{A} , where $|\mathcal{A}| = M = 2^m$

$$s_n = \Phi[\tilde{\mathbf{c}}_n], \quad n = 1, \dots, N_s. \quad (3)$$

Finally, reference symbols (pilots) are interleaved with the payload \mathbf{s} so the sequence of transmitted symbols can be presented as

$$\mathbf{x} = [x_0, x_1, \dots, \underset{\uparrow}{x_{L-1}}, \underset{\uparrow}{x_L}, x_{L+1}, \dots, \underset{\uparrow}{x_N}] \quad (4)$$

where we indicate with arrows the pilot symbols $x_{lL}, l = 0, \dots, F$ and $x_n, n \neq lF$ are payload symbols from \mathbf{s} . That is, $x_{n'} = s_n, n = 1, \dots, N_s$ where the mapping $n \rightarrow n'$ allows to index the symbols in \mathbf{x} by skipping the pilots. We will use the values of L which satisfy $N_s = F(L - 1)$ for integer F .

Similarly, the BICM decoding is carried out in two steps [9, Chap. 1.4]

- 1) *Phase tracking and demodulation*: consists in finding the marginal conditional probability of the coded bits

$$\Pr\{c_{n,k} = c | \mathbf{y}\} \quad (5)$$

$$\propto \sum_{a \in \mathcal{A}_{k,c}} \Pr\{s_n = a | \mathbf{y}\}, \quad c \in \{0, 1\}, \quad (6)$$

where $\mathbf{y} = [y_0, \dots, y_N]$ gathers all the channel outcomes and

$$\mathcal{A}_{k,c} = \{\Phi[\mathbf{c}], \mathbf{c} = [c_1, \dots, c_{k-1}, c, c_{k+1}, \dots, c_m]\} \quad (7)$$

is a sub-constellation comprising only the symbols labeled by the bit with value c at the position k ; \propto will be used in the text to indicate that the distributions are defined up to a multiplicative factor which is independent of the distribution argument (here c).

Since $s_n = x_{n'}$, to obtain (5) we have to calculate the conditional distribution of the symbols x_n

$$P_n(a) \triangleq \Pr\{x_n = a | \mathbf{y}\}, \quad a \in \mathcal{A}; \quad (8)$$

this operation involves marginalization over the phase θ_n and the transmitted symbols

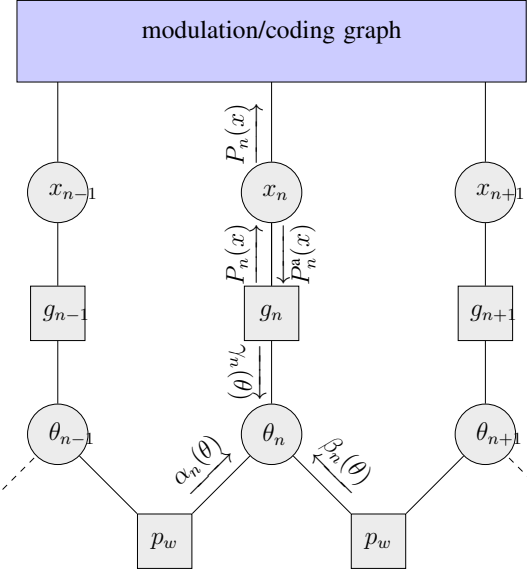


Fig. 1. Graph defining the relationship between the variables in the phase tracking problem; the messages exchanged between the nodes are shown together with the arrows indicating the direction of the exchange.

$x_t, t \neq n$, and is a “phase tracking” since, as a byproduct of (8), we will obtain the distribution of the phase $f(\theta_n | \mathbf{y})$.

2) *Soft-input decoding*: using (8) and (5) we calculate the logarithmic likelihood ratios (LLRs) for the coded bits $c_{n,k}$

$$\begin{aligned} \lambda_{n,k} &= \log \frac{\Pr \{c_{n,k} = 1 | \mathbf{y}\}}{\Pr \{c_{n,k} = 0 | \mathbf{y}\}} \\ &\approx \max_{a \in \mathcal{A}_{k,1}} \hat{P}_{n'}(a) - \max_{a \in \mathcal{A}_{k,0}} \hat{P}_{n'}(a), \end{aligned} \quad (9)$$

where we applied the max-log simplification using the log-probability, $\hat{P}_n(a) = \log P_n(a)$; the logarithmic domain simplifies implementation and will appear in all parametric derivations; we use again the mapping $n \rightarrow n'$.

The LLRs are fed to the binary decoder which operates in abstraction of how they were calculated.

III. PHASE TRACKING

Our goal now is to find $P_n(a)$ exploiting the relationships between the involved random variable.

As in [1], [6], we show in Fig. 1 a graph which captures this relationship: the squares represent the functions taking as arguments the variables which, in turn, are represented by the directly connected circles. In particular

$$g_n(\theta_n, x_n) \propto \exp\left(-\text{snr}\left|y_n - x_n e^{j\theta_n}\right|^2\right) \quad (10)$$

corresponds to the relationship defined in (1) and

$$p_w(\theta_n, \theta_{n+1}) = \omega(\theta_n - \theta_{n+1}) \quad (11)$$

corresponds to (2) and thus $\omega(\theta) = \mathcal{N}(\theta; 0, \sigma_w^2)$, where the wrapped Gaussian distribution is defined as

$$\mathcal{N}(\theta; m, v) = \frac{1}{\sqrt{2\pi v}} \sum_{k=-\infty}^{\infty} \exp\left(-\frac{(\theta - m - k2\pi)^2}{2v}\right). \quad (12)$$

In Fig. 1 we also show a shaded rectangle labeled as “modulation/coding graph”; it also contains a graph which describes the relationship $x \rightarrow s \rightarrow c \rightarrow b$, and its knowledge is used for the demodulation (to implement (9)) and for the decoding.

If the phase tracking has to be carried out and no decoding was not yet executed, the payload symbols x_n are assumed to be i.i.d., with non-informative distribution, i.e., $P_n^a(a) \propto 1$. In a case we would like to perform the joint decoding/demodulation/phase tracking, as done, e.g., in [1] [6] [4], we use $P_n^a(x)$ obtained from the decoding results.

Thus, from the point of view of the phase tracking, the relationships induced by the modulation/coding graph are summarized by $P_n^a(a)$. As a direct consequence, the graph we deal with in Fig. 1 is a tree, i.e., contain no loops. Therefore, the efficient marginalization can be done exactly by the MP algorithm as follows [1], [5], [6]

$$P_n(a) \propto \int_{-\pi}^{\pi} \alpha_n(\theta) \beta_n(\theta) g_n(\theta, a) d\theta, \quad a \in \mathcal{A}, \quad (13)$$

where

$$\alpha_n(\theta) \propto (\alpha_{n-1}(\theta)\gamma_{n-1}(\theta)) * \omega(\theta) \quad (14)$$

$$\beta_n(\theta) \propto (\beta_{n+1}(\theta)\gamma_{n+1}(\theta)) * \omega(\theta) \quad (15)$$

$$\gamma_n(\theta) \propto \sum_{a \in \mathcal{A}} P_n^a(a) g_n(\theta, a), \quad (16)$$

are (proportional to) the marginal distributions of the phase θ_n conditioned, respectively, on y_0, \dots, y_{n-1} , on y_{n+1}, \dots, y_N , and on y_n .¹ All the distributions of the phase are periodic and so is the convolution in (14) and (15).

IV. PARAMETRIC MESSAGE PASSING

The operations (13)-(16) which allow us to calculate $P_n(a)$ may be implemented on the discretized versions of the distributions $\alpha_n(\theta)$, $\beta_n(\theta)$, and $\gamma_n(\theta)$ defined over the samples of $\theta \in (-\pi, \pi]$. In such a DMP the multiplications and additions are straightforward to implement and the convolution is efficiently implemented via fast Fourier transform (FFT).

However, to ensure sufficient precision, large number of samples, N_θ , may be necessary implying possibly a large complexity and storage burden.² Therefore, many previous works have gone in the direction of parametric representation of the involved periodic distributions. Then, instead of tracking the samples in DMP, we only need to track (a few) parameters which

¹That is,

$$\alpha_n(\theta) \propto f(\theta_n | y_0, \dots, y_{n-1}) \quad (17)$$

$$\beta_n(\theta) \propto f(\theta_n | y_{n+1}, \dots, y_N) \quad (18)$$

$$g_n(\theta, a) \propto f(\theta_n | y_n, a) \quad (19)$$

and thus the integrand in (13) is the posterior distribution of the phase

$$f(\theta_n | \mathbf{y}, a) \propto \alpha_n(\theta)\beta_n(\theta)g_n(\theta, a) \quad (20)$$

²The number of samples, N_θ , required to represent the distributions over the interval of length 2π and to ensure the accuracy of the MP, (14)-(16), is difficult to estimate. Nevertheless, all the distributions involved in the MP should be represented without significant loss of accuracy so the sampling step should decrease when the spectrum support of the distributions increases.

Approximating the distributions by Gaussians, the precision (inverse of the variance) is proportional to the spectral support. Thus, observing that the precision of $g_n(\theta, a)$ increases with the SNR, see also (24)-(25), and the precision of $\omega(\theta)$ decreases with σ_w^2 , we may conclude that the number of samples will grow when we increase the SNR or when we decrease the phase-noise level. These operational conditions are also required to transmit reliably high-order constellations, which is where the impact of the DMP complexity will be the most notable. In such a case, the simplification may be sought by limiting the period over which the distribution must be represented [2].

represent the distributions. We thus have to find a family of the distributions, \mathcal{F} , on which the operations defined in (13)-(16) are easily dealt with.

In other words, if $\alpha_n(\theta), \beta_n(\theta), \gamma_n(\theta), \omega(\theta) \in \mathcal{F}$ and \mathcal{F} is closed under multiplication and convolution, the parametric MP will be immediately obtained. This condition, however, does not materialize with the most popular circular distributions such as the wrapped Gaussian distributions or the Tikhonov distributions [10]. Namely, the space of wrapped Gaussian distributions is not closed under multiplications, while the Tikhonov space is not closed under convolution. Thus, independently of the choice we make, approximations will be necessary.

A. Tikhonov distributions

In this work we consider a family of Tikhonov distributions which were already used, e.g., in [1] [11] [5], and are defined as

$$\mathcal{T}(\theta; z) = \frac{e^{\Re[ze^{-j\theta}]}}{2\pi I_0(|z|)}, \quad (21)$$

where $\Re[\cdot]$ denotes the real part and $I_0(\cdot)$ is the zero-th order modified Bessel function; z is a complex parameter whose phase is the circular mean of the underlying variable and the value of $|z|$ is, approximatively, a measure of precision [10].

The closeness of \mathcal{F} under multiplication is then obvious

$$\mathcal{T}(\theta; z_1)\mathcal{T}(\theta; z_2) = \frac{I_0(|z_1 + z_2|)}{2\pi I_0(|z_1|)I_0(|z_2|)}\mathcal{T}(\theta; z_1 + z_2), \quad (22)$$

while the convolution with the Gaussian, appearing in (14) and (15), must be treated via approximations as done before [1, Appendix] and also explained using the concept of a circular moment matching (CMM) in Appendix C

$$\mathcal{T}(\theta; z) * \mathcal{N}(\theta; 0, \sigma_w^2) \approx \mathcal{T}\left(\theta; \frac{z}{1 + v|z|}\right). \quad (23)$$

We also note that $g_n(\theta, a) \in \mathcal{F}$, that is, we can write (10) as

$$g_n(\theta, a) \propto e^{\xi_{g,n}(a)} \mathcal{T}(\theta; z_{g,n}(a)) \quad (24)$$

$$z_{g,n}(a) = 2 \frac{y_n a^*}{N_0} \quad (25)$$

$$\xi_{g,n}(a) = -\frac{|a|^2}{N_0} + \hat{I}_0(|z_{g,n}(a)|), \quad (26)$$

where, to avoid numerical issues due to the exponential grows of $I_0(\cdot)$ we use its log-version

$$\hat{I}_0(x) = \log I_0(x) = x + \Delta(x), \quad (27)$$

with $\Delta(x)$ being the log-domain corrective factor.³

Instead of Tikhonov family we might opt for the wrapped Gaussians (12) but i) to take care of their periodic nature, particular attention is required when dealing with multiplication [10, Sec. II.B],⁴ ii) comparing to the Tikhonov distributions, Gaussians are less well suited to represent the uniform or almost-uniform distributions of the phase, and iii) we have to start approximations already when representing $g_n(\theta, a)$ which is naturally represented by a Tikhonov distribution in (24); this can be done, of course, e.g., as in [6], but requires introduction of additional layer of approximations before the MP is derived.

B. Approximation of $\gamma_n(\theta)$

The main need for approximations stems from the presence of $\gamma_n(\theta)$ which, being a mixture of Tikhonov distributions, see (16), does not belong itself to \mathcal{F} . Namely,

$$\gamma_n(\theta) = \sum_{a \in \mathcal{A}} e^{\eta_{g,n}(a)} \mathcal{T}(\theta; z_{g,n}(a)), \quad (28)$$

$$\eta_{g,n}(a) = -\frac{|a|^2}{N_0} + \hat{I}_0(|z_{g,n}(a)|) + \hat{P}_n^a(a), \quad (29)$$

³The approximation $\Delta(x) \approx -\frac{1}{2} \log(2\pi x)$ is tight for large x [5, Eq. (96)] [7, Eq. (18)] but does not apply for small arguments because $\Delta(0) = 0$. Thus, for a better accuracy, $\Delta(x)$ may be implemented via lookup table. On the other hand, it is also possible to simply set $\Delta(x) \approx 0$.

⁴This aspect is not always emphasized in the literature: in some works, the Gaussian distributions are used without explicit wrapping. Ignoring the circularity, it produces an apparent closeness under multiplication but may lead to interpretation errors when “locking” on the wrong phase, see example in [10, Fig. 1].

where we again use $\hat{P}_n^a(a) = \log P_n^a(a)$ because the logarithmic representation simplifies the implementation.

To deal with this issue, Colavolpe, Barbieri and Caire [1] proposed to approximate $\gamma_n(\theta)$ with $\tilde{\gamma}_n(\theta) \in \mathcal{F}$ by, first matching a Gaussian to $f(y_n|\theta_n, a) \propto g_n(\theta, a)$ from which a Tikhonov distribution was derived as [1, Sec. IV.B]

$$\tilde{\gamma}_n(\theta) = \mathcal{T}(\theta; z_{\tilde{\gamma},n}) \quad (30)$$

$$z_{\tilde{\gamma},n} = \begin{cases} z_{g,n}(x_n) & \text{if } n = lL \\ 2\frac{y_n m_n^*}{N_0 + v_n}, & \text{if } n \neq lL \end{cases} \quad (31)$$

where

$$m_n = \sum_{a \in \mathcal{A}} a P_n^a(a), \quad v_n = \sum_{a \in \mathcal{A}} |a|^2 P_n^a(a) - |m_n|^2, \quad (32)$$

are the mean and the variance of x_n .

The approximation is needed only for the payload positions, $n \neq lL$. For the pilots $x_n, n = lL$, we have $\gamma_n(\theta) = g_n(\theta, x_n)$ so we can use directly the parameter of the Tikhonov distribution $z_{g,n}(x_n)$.

This Gaussian approximation (GA) approach was often reused in the literature, e.g., [11] [7] [4] as the integral part of the CBC algorithm.

On the other hand, recognizing that the distribution (28) is circular, instead of the GA we may apply the CMM. It relies on minimization of the Kullback-Leibler (KL) distance between $\tilde{\gamma}_n(\theta)$ and the mixture $\gamma_n(\theta)$, and changes the way the parameter $z_{\tilde{\gamma},n}$ is calculated

$$\tilde{\gamma}_n(\theta) = \mathcal{F} \left[\sum_{a \in \mathcal{A}} e^{\eta_{g,n}(a)} \mathcal{T}(\theta; z_{g,n}(a)) \right], \quad (33)$$

$$z_{\tilde{\gamma},n} = \begin{cases} z_{g,n}(x_n) & \text{if } n = lL \\ \text{CMM} \left[\eta_{g,n}(a), z_{g,n}(a) \mid a \in \mathcal{A} \right] & \text{if } n \neq lL. \end{cases} \quad (34)$$

where, again, only the payload symbols, $x_n, n \neq lL$ require the approximation. With a slight abuse of notation we use $\mathcal{F}[\cdot]$ to denote the operator which “projects” $\gamma_n(\theta)$ onto the Tikhonov family \mathcal{F} . As a result we obtain the distribution with the parameter $z_{\tilde{\gamma},n}$ which depends only on $\eta_{g,n}(a)$ and $z_{g,n}(a)$, where $a \in \mathcal{A}$; this dependence is defined in closed-form by a function

CMM[.] shown in Appendix A.

C. Colavolpe–Barbieri–Caire algorithm [1]

Next, if all the distributions are from the Tikhonov family, i.e., $\alpha_n(\theta) = \mathcal{T}(\theta; z_{\alpha,n})$ and $\beta_n(\theta) = \mathcal{T}(\theta; z_{\beta,n})$, using $\tilde{\gamma}_n(\theta)$ instead of $\gamma_n(\theta)$ in (22) and (23), we obtain the following parametric MP :

$$z_{\alpha,0} = 0, \quad (35)$$

$$z_{\alpha,n} = \frac{z_{\alpha,n-1} + z_{\tilde{\gamma},n-1}}{1 + |z_{\alpha,n-1} + z_{\tilde{\gamma},n-1}| \sigma_w^2}, \quad n = 1, \dots, N-1 \quad (36)$$

$$z_{\beta,N} = 0, \quad (37)$$

$$z_{\beta,n} = \frac{z_{\beta,n+1} + z_{\tilde{\gamma},n+1}}{1 + |z_{\beta,n+1} + z_{\tilde{\gamma},n+1}| \sigma_w^2}, \quad n = N-1, \dots, 1, \quad (38)$$

which is exactly equivalent to the CBC algorithm defined in [1, Eq. (36)–(37)] and is provided for completeness and as a starting point for the discussion.

Using (22) and (24)–(26) in (13), the “extrinsic” symbol probabilities are also calculated as [1, Eq. (35)]

$$P_n(a) \propto \int_0^{2\pi} \mathcal{T}(\theta; z_{\Sigma,n}(a)) \frac{e^{\xi_{g,n}(a)} I_0(|z_{\Sigma,n}(a)|)}{I_0(|z_{g,n}(a)|)} d\theta, \quad (39)$$

$$\hat{P}_n(a) = -\frac{|a|^2}{N_0} + \hat{I}_0(|z_{\Sigma,n}(a)|), \quad (40)$$

$$z_{\Sigma,n}(a) = z_{\alpha,n} + z_{\beta,n} + 2\frac{y_n a^*}{N_0}, \quad (41)$$

and the log-probability $\hat{P}_n(a) = \log P_n(a)$ should be next used in (9).

Due to its simplicity, the CBC algorithm (35)–(38), should be treated as a “canonical” solution to the problem of phase tracking in the sense that it is can be implement without additional assumptions. This explains the considerable attention it received up to now.

Before going further, we note that the difference between the original formulation of the CBC algorithm in [1] and this work appears in the way the approximate distribution $\tilde{\gamma}_n(\theta)$ is obtained, that is, whether we opt for the GA (30)–(32), or we use the CMM from (34).

Although the CMM was already used in the context of the phase tracking by [5], we are not aware of it being applied directly in the CBC algorithm. And while the implementation of the

function CMM[.] is less straightforward⁵ than the GA shown in (30)-(32), we will soon compare the CMM to the GA and show the obvious advantage produced by the former.

An important observation, already made e.g., in [5, Sec. I] or [7, Sec. IV], is that, using a non-informative prior $\hat{P}^a(a) \propto 0$, the approximation $\tilde{\gamma}_n(\theta)$ is also non-informative for the payload symbols; that is, $z_{\tilde{\gamma},n} = 0, n \neq lL$.⁶

Since then, the only useful information is obtained from the non-zero $z_{\tilde{\gamma},n}$, that is, from the pilots, the MP in (35)-(38), may be then seen as a *pilot-only* based recursive estimation of the phase. And it is independent of the form of the constellation \mathcal{A} used to modulate the payload symbols.

This is why, in order to exploit the form of the constellation \mathcal{A} , the CBC phase tracking is put in the “decoding-loop”. Known also as the joint phase tracking and decoding, it consists in alternate execution of i) the MP (35)-(38) and ii) the demodulation/decoding; the latter, providing an informative prior $\hat{P}_n^a(a)$ on the payload symbols, improves the phase tracking, see e.g., [1] [11] [4].

D. Scheduling and complexity

It may, therefore, be useful to define a *scheduling* which specifies the number of iteration the LDPC decoder executes before its outputs are transformed into $\hat{P}_n(a)$ and used again by the phase tracking MP.

Let the scheduling defined by $\{I_{\text{loop}} \times I_{\text{dec}}\}$ means the following: after each passage of the CBC phase tracking, the decoder executes I_{dec} elementary decoding iterations⁷, then the phase tracking is implemented again and the results are used by the decoder executing I_{dec} elementary decoding iterations. This is repeated I_{loop} times so the total number of decoding iterations is given by $I_{\text{dec}}^{\Sigma} = I_{\text{loop}} \cdot I_{\text{dec}}$.

The scheduling from [1] is defined by $\{200 \times 1\}$ meaning that the phase-tracking was executed $I_{\text{loop}} = 200$ times and, each phase-tracking was followed by one elementary decoding iterations; the total number of decoding iterations if thus $I_{\text{dec}}^{\Sigma} = 200$.

⁵Approximations of non-linear functions are involved, see Appendix A and Appendix B.

⁶If the GA (30)-(32), is used, this is true, if the constellation \mathcal{A} is zero mean, which is obvious from (32). On the other hand, if the CMM approach is used, this is true for constellations \mathcal{A} which may be decomposed into constant modulus zero-mean sub-constellations; the demonstration is easy and omitted for sake of space. For the most popular constellations such as M -quadrature amplitude modulation (QAM), both conditions hold.

⁷Defined as one check-nodes message update and one bit-nodes message update.

A “one-shot” phase tracking is denoted by the scheduling $\{1 \times I_{\text{dec}}^\Sigma\}$, and means that the phase tracking is carried out once and then all the decoding iterations are executed.

There are clearly many other possibilities to schedule the operations and they may affect the performance and the complexity. However, caution should be applied when talking about the implementation complexity because it is difficult to compare different operations: counting the additions/multiplications may be misleading especially when targeting implementation on the specialized circuits.

For example, the operations necessary in the CMM do not have the same implementation “complexity” as those required by the MP (35)-(38); and it is difficult to compare any of these to the operations required by the elementary decoding iteration. However, when operations are of the same type, they can be compared and provide a general idea about the complexity.

E. Example: Phase tracking reference results

The test scenario that will be reused later considers transmission based on 16-QAM constellation with Gray mapping [9, Sec. 2.5.2]; the proprietary LDPC encoder with the rate $R = \frac{7}{8}$ is applied to the block of $N_b = 4032$ bits. The pilot symbols are pseudo-randomly drawn from a 4-QAM constellation; the pilot spacing is set to $L = 25$ which allows us to place $L - 1 = 24$ payload symbols between pilots, see (4), so dummy symbols are not needed to fill the frame of transmitted symbols \mathbf{x} ; we thus have $F = 43$ pilots and total $N = 1051$ symbols. The noise level is $\sigma_w^2 = 0.01$.

The PER, shown in Fig. 2 is estimated after transmitting 10^5 blocks or after occurrence of 100 blocks in error, whichever comes first. In all cases the total number of decoding iterations is or $I_{\text{dec}}^\Sigma = 10$ (solid markers) or $I_{\text{dec}}^\Sigma = 30$ (hollow markers); the decoding is based on the min-sum algorithm.⁸

The DMP is implemented using $N_\theta = 64$ samples and its PER curve is the performance limit for all “one-shot” phase tracking algorithms, i.e., those defined by the scheduling $\{1 \times I_{\text{dec}}\}$.

The curve “All-pilots” is obtained assuming that, during the phase-tracking, all the symbols in \mathbf{x} are pilots. This correspond to a situation when the output of the decoder provides highly

⁸With scaling of the check-nodes messages by a constant factor equal to $\rho = 0.7$, see [12]; then, a fraction of dB loss was observed when comparing to the sum-product algorithm in the AWGN channel.

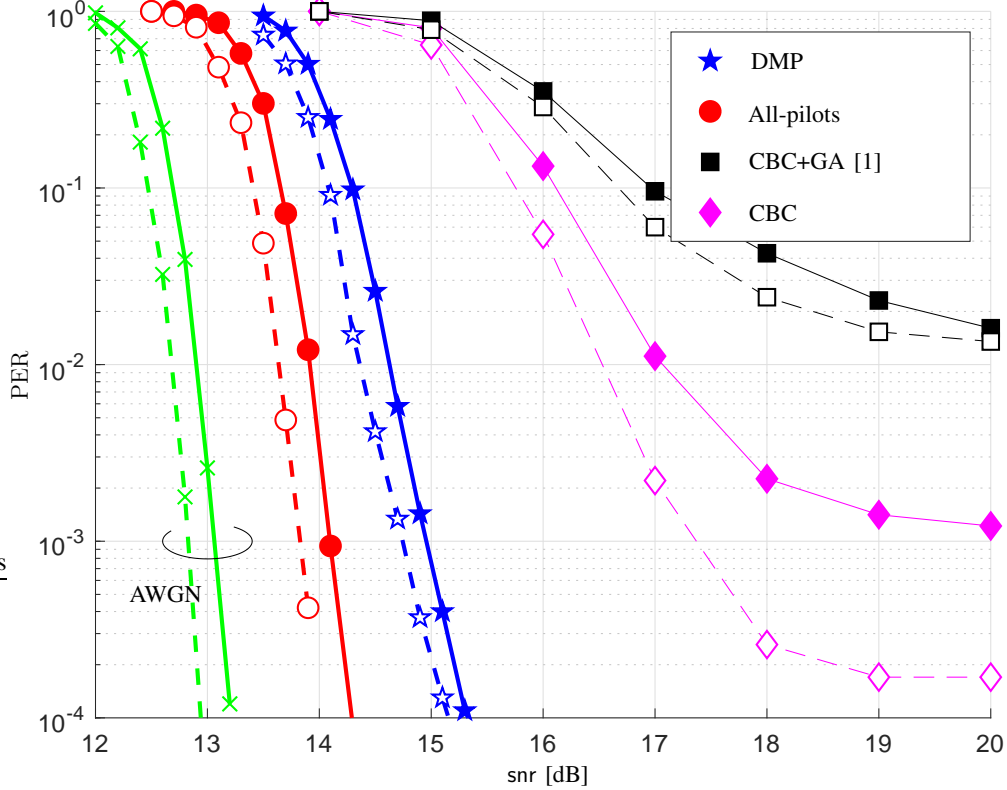


Fig. 2. PER vs. SNR obtained using CBC algorithm with the projection based on the Gaussian approximation (GA) originally proposed in [1] (CBC+GA) or, on the circular moment matching (CMM) explained in Appendix A (CBC), both shown for the scheduling $\{I_{\text{dec}} \times 1\}$ with $I_{\text{dec}} = 10$ (filled markers, solid lines) and $I_{\text{dec}} = 30$ (hollow markers, dashed lines); the encoding rate of the LDPC is $R = \frac{7}{8}$. The discretized message passing (DMP) is implemented using $N_\theta = 64$ samples, the “AWGN” curve assumes no phase noise, and “All pilots” curve is the performance limits for any joint phase tracking and decoding, see explanation in Sec. IV-E.

reliable information about the bits which gives certainty about the symbols x (that is, $P_n^a(a) \approx 1$ for $a = x_n$); these, in turn, become de facto pilots allowing for the best possible phase tracking.

Then, when calculating $\hat{P}_n(a)$, the only uncertainty about the symbol x_n is due to the AWGN noise and the residual phase noise – this part of it which cannot be estimated from other symbols $x_l, l \neq n$. The “All-pilots” curve is a performance limit for any joint phase-tracking and demodulation/decoding algorithms. If the DMP is too complex to implement, the “All-pilots” curve may be treated as the proxy for the DMP.

On the other hand, the “AWGN” curve corresponds to a hypothetical scenario when the phase-noise is removed and we only deal with the AWGN. Such results are unattainable no matter how sophisticated the phase-tracking and decoding strategy are, and we show them to illustrate

the impact of the phase noise.

As for the CBC phase tracking, we observe the following

- The PER of the original CBC algorithm from [1] (CBC+GA) tends to saturate for high SNR, i.e., where the phase noise dominates the AWGN. This effect seems to be difficult to remove by increasing the number of iterations. We attribute this behaviour, observed already e.g., in [6, Fig. 8], to the scheduling, where, after each decoding iteration, $\tilde{\gamma}_n(\theta)$ is estimated afresh even if the first decoding iterations do not provide reliable estimates of the coded bits. This, in turn, may yield unreliable $\hat{P}^a(a)$, hence unreliable $\tilde{\gamma}_n(\theta)$ which, in turn stalls the convergence.
- The notable difference between the original CBC algorithm (CBC+GA) and the CBC algorithm based on the CMM (CBC) emphasizes the importance of the approximations we make in the phase tracking: by using the CMM, we significantly lower the operational SNR⁹ and the error floor in the high SNR. Thus, all the remaining results are based on the CMM.
- Irrespectively of the valuable improvement due to the application of the CMM, the qualitative behaviour of the CBC algorithms is the same: the error floor appears in the PER curve and the gap to the DMP remains large even when we increase the number of iterations. We hasten to say, that it is possible that the error floor occurs also for the DMP but it may be difficult to attain without excessively heavy simulations.

V. EXPECTATION PROPAGATION: SELF-ITERATIONS IN THE PHASE-TRACKING

The example in Sec. IV-E, showing the improvement in performance obtained by replacing the GA proposed originally in [1] with the CMM, demonstrates that the reliable phase-tracking results may improve the performance significantly.

Along the same light of thought, comparing the performance of the CBC algorithm with the one-shot phase-tracking of the DMP, indicates that satisfactory solutions may be obtained without relying on the decoders' feedback. Therefore, our goal now is to develop a reliable and "standalone" (which can operate without decoder's feedback) phase tracking by exploiting the form of the constellation \mathcal{A} .

⁹The SNR necessary to attain a given PER target, e.g., for $\text{PER}_t = 10^{-2}$, the SNR decreases by 2dB.

A similar idea was followed in [5] where the original mixture $\gamma_n(\theta)$ (16) was used in (14) and (15) and the results of multiplication $\alpha_n(\theta)\gamma_n(\theta)$ and $\beta_n(\theta)\gamma_n(\theta)$ were projected on the space of Tikhonov mixtures \mathcal{F} . In this way, the projection $\mathcal{F}[\cdot]$ is moved “inside” the MP; this improves the performance but, requires more projections and thus increases the complexity comparing to the CBC algorithm. Similar principle was explored in [6] but using the Gaussian family \mathcal{F} .

Here, we follow the idea of the CBC algorithm motivated by the extreme simplicity of the forward-backward MP (35)-(38) which amounts to non-linear recursive filtering. Thus, unlike [5] [6], rather than moving the projection inside the MP, we want to enhance the approximations $\tilde{\gamma}_n(\theta)$ and preserve the structure of the MP (35)-(38).

To do this, we will improve $\tilde{\gamma}_n(\theta)$ iteratively; this will be done with “self-iterations”, that is without any help from the decoder: the priors $\hat{P}^a(a)$ will not change during the self-iterations.

To explain why this can be done we note that, although the phase tracking MP is defined on the tree (graph) that is known to yield the optimal solution in one run (backward-forward processing), this is only true for the DMP which tracks the entire (discretized) distributions. On the other hand, the MP in the CBC algorithm is based on approximated distribution $\tilde{\gamma}_n(\theta)$ and, therefore, such a guarantee of optimality does not exist.

We follow here the EP idea [8, Ch. 3.2] which addresses the very problem of using approximate distributions in the MP. We will apply the projection $\mathcal{F}[\cdot]$ many times (iteratively) taking into account the results obtained in previous iterations. Since most of the resulting operations are almost identical to those we already defined in the CBC algorithm, we will use the parenthesized superscript (i) to denote the variables/functions obtained in the i -th iteration, where $i = 1, \dots, I_{\text{ep}}$ and I_{ep} is the maximum number of EP iterations.

A. Expectation Propagation for the Phase Tracking

The EP applied to our problem relies on the following idea: in the iteration i , we find the approximation $\tilde{\gamma}_n^{(i)}(\theta)$ using the distributions $\alpha_n^{(i-1)}(\theta)$ and $\beta_n^{(i-1)}(\theta)$ calculated in the previous iterations. This is done by matching the posterior distribution of θ_n , that would be obtained using $\tilde{\gamma}_n^{(i)}(\theta)$ to the one calculated from the original distribution $\gamma_n(\theta)$

$$\begin{aligned} \tilde{\gamma}_n^{(i)}(\theta) & \left(\alpha_n^{(i-1)}(\theta) \beta_n^{(i-1)}(\theta) \right) \\ & \approx \gamma_n(\theta) \left(\alpha_n^{(i-1)}(\theta) \beta_n^{(i-1)}(\theta) \right) \end{aligned} \quad (42)$$

and requires the projection operation, $\mathcal{F}[\cdot]$ to be applied to both sides of (42).

Since the left-hand side (l.h.s.) contains the three terms from the family \mathcal{F} , it is not affected by the projection (remember, the product of the Tikhonov distributions is also a Tikhonov distribution), we obtain

$$\tilde{\gamma}_n^{(i)}(\theta) \propto \frac{\mathcal{F}[\gamma_n(\theta)(\alpha_n^{(i-1)}(\theta)\beta_n^{(i-1)}(\theta))]}{\alpha_n^{(i-1)}(\theta)\beta_n^{(i-1)}(\theta)}. \quad (43)$$

Of course, for $i = 1$, we deal with non-informative distributions $\alpha^{(0)}(\theta) \propto 1$ and $\beta^{(0)}(\theta) \propto 1$, which reduces (43) to $\tilde{\gamma}_n^{(1)}(\theta) = \mathcal{F}[\gamma_n(\theta)]$; this is what was done in Sec. IV, i.e., $\tilde{\gamma}_n^{(1)}(\theta)$ is the same as $\tilde{\gamma}_n(\theta)$ obtained in (33).

For $i > 1$, the informative distributions, $\alpha_n^{(i-1)}(\theta)$ and $\beta_n^{(i-1)}(\theta)$ are available so we have to calculate the right-hand side (r.h.s.) of (42)

$$\gamma_n(\theta)(\alpha_n^{(i-1)}(\theta)\beta_n^{(i-1)}(\theta)) = \sum_{a \in \mathcal{A}} e^{\eta_{\Sigma,n}^{(i-1)}(a)} \mathcal{T}(\theta; z_{\Sigma,n}^{(i-1)}(a)), \quad (44)$$

where, with proper sup-indexing in (41), we have $z_{\Sigma,n}^{(i-1)}(a) = z_{\alpha,n}^{(i-1)} + z_{\beta,n}^{(i-1)} + z_{g,n}(a)$ and

$$\eta_{\Sigma,n}^{(i-1)}(a) = -\frac{|a|^2}{N_0} + \hat{I}_0(|z_{\Sigma,n}^{(i-1)}(a)|) + \hat{P}_n^a(a) \quad (45)$$

$$= \hat{P}_n^{(i-1)}(a) + \hat{P}^a(a) \quad (46)$$

represents the posterior log-probability of the symbols obtained in the iteration $i - 1$.

Using (44) in (43) yields

$$\tilde{\gamma}_n^{(i)}(\theta) = \mathcal{T}(\theta; z_{\tilde{\gamma},n}^{(i)}) \quad (47)$$

$$\propto \frac{\mathcal{F}\left[\sum_{a \in \mathcal{A}} e^{\eta_{\Sigma,n}^{(i-1)}(a)} \mathcal{T}(\theta; z_{\Sigma,n}^{(i-1)}(a))\right]}{\mathcal{T}(\theta; z_{\alpha,n}^{(i-1)} + z_{\beta,n}^{(i-1)})} \quad (48)$$

$$= \frac{\mathcal{T}(\theta; z_{\text{post},n}^{(i)})}{\mathcal{T}(\theta; z_{\alpha,n}^{(i-1)} + z_{\beta,n}^{(i-1)})}, \quad (49)$$

where

$$z_{\text{post},n}^{(i)} = \text{CMM}\left[\eta_{\Sigma,n}^{(i-1)}(a), z_{\Sigma,n}^{(i-1)}(a) \mid a \in \mathcal{A}\right] \quad (50)$$

and thus

$$z_{\tilde{\gamma},n}^{(i)} = z_{\text{post},n}^{(i)} - (z_{\alpha,n}^{(i-1)} + z_{\beta,n}^{(i-1)}). \quad (51)$$

B. Pitfalls and solutions

The elegant formulation of the EP is indeed appealing but occasionally runs into difficulty due to the division of the distributions in (49), or equivalently, due to subtraction of the coefficients in (51). The existence of such a problem has been acknowledged in [8, Sec. 3.2] in the context of the Gaussian EP, where the division of the distributions may yield a “Gaussian” with negative variance, see also [13, Sec. IV.B] [14, Sec. IV.A]. Such results are usually uninterpretable so the workarounds are needed.

In the context of the Tikhonov distributions $\mathcal{T}(\theta; z)$ defined by a complex parameter z , the purely numerical issue of invalid parameters (such as a negative variance in the Gaussian case) is avoided but the problem remains. To understand intuitively its source and devise a solution, we may look at the scenario where the problems materialize.

Example 1 (Pitfalls of EP): Assume that

- The circular means of the approximate posterior distribution, $\mathcal{T}(\theta; z_{\text{post},n}^{(i)})$ and of the “extrinsic” distribution (defined by the product $\alpha_n^{(i-1)}(\theta)\beta_n^{(i-1)}(\theta)$) coincide, that is, $\angle z_{\text{post},n}^{(i)} = \angle(z_{\alpha,n}^{(i-1)} + z_{\beta,n}^{(i-1)})$; (remember, the phase $\angle z_{\text{post},n}^{(i)}$ defines the circular mean); and that
- The variance of the posterior distribution is larger than the variance of the extrinsic distribution, i.e., $|z_{\text{post},n}^{(i)}| < |z_{\alpha,n}^{(i-1)} + z_{\beta,n}^{(i-1)}|$; this may occur because the distribution in the argument of $\mathcal{F}[\cdot]$ in (48) is obtained multiplying the extrinsic distribution $\mathcal{T}(\theta; z_{\alpha,n}^{(i-1)} + z_{\beta,n}^{(i-1)})$ with a mixture $\gamma_n(\theta)$; the variance of the resulting mixture (and thus of its projection result as well) may be larger than the variance of the extrinsic distribution.

Then, carrying out the subtraction in (51) we will obtain

$$z_{\tilde{\gamma},n}^{(i)} = (|z_{\text{post},n}^{(i)}| - |z_{\alpha,n}^{(i-1)} + z_{\beta,n}^{(i-1)}|) e^{j\angle z_{\text{post},n}^{(i)}} \quad (52)$$

$$= |z_{\tilde{\gamma},n}^{(i-1)}| e^{j(\angle z_{\text{post},n}^{(i)} + \pi)}. \quad (53)$$

That is, the circular mean of the new distribution $\mathcal{T}(\theta; z_{\tilde{\gamma},n}^{(i)})$ will be in disagreement (by the largest possible value of π) with the mean of the posterior and extrinsic distributions obtained

from the previous iteration. Such a results, being an artefact of the way the EP is defined [8, Sec. 3.2] is clearly counterintuitive and simply wrong.

This problem, characteristic of the EP occurs in $\tilde{\gamma}_n(\theta)$ and, propagating via the MP, affects $\alpha_n(\theta)$ and $\beta_n(\theta)$.

Heuristics were devised for the Gaussian EP where the problem is clearly identified, i.e., the variance of the distributions after division becomes negative. For example, [8, Sec. 3.2] constrains the variance to be positive, while other proposed to identify the problematic cases (i.e., the negative variance) and then, if necessary i) eliminate the division of the distributions [13, Sec. IV.B], which here would mean $z_{\tilde{\gamma},n}^{(i)} = z_{\text{post},n}^{(i)}$, or ii) remove the update [14, Sec. IV.A], i.e., $z_{\tilde{\gamma},n}^{(i)} = z_{\tilde{\gamma},n}^{(i-1)}$.

On the other hand, instead of testing for the compliance with our prior requirements (that are not necessarily obvious to define), we might “smooth” the obtained parameters via recursive filter [14, Sec. IV.A], which would mean replacing (51) with

$$z_{\tilde{\gamma},n}^{(i)} = \zeta \left(z_{\text{post},n}^{(i)} - z_{\alpha,n}^{(i-1)} - z_{\beta,n}^{(i-1)} \right) + (1 - \zeta) z_{\tilde{\gamma},n}^{(i-1)} \quad i = 2, \dots, I_{\text{ep}}, \quad (54)$$

where $\zeta < 1$ must be chosen heuristically to strike a balance between the new solution and the history accumulated in the previous estimate. In this way we avoid rapid changes in the parameters $z_{\tilde{\gamma},n}^{(i)}$, providing a sort of regularization which robustifies the final solution. Note that the smoothing is not necessary in the first iteration, $i = 1$, which is based solely on the information obtained from the pilots and from the decoder (if such option is allowed).

We applied this smoothing solution in our numerical experiments, and found $\zeta \approx 0.4$ yielding satisfactory results.

C. Summary of the algorithm

The entire algorithm is now summarized as Algorithm 1 where for simplicity we defined the set of indices to the payload symbols and to the pilots as

$$\mathbb{N}_{\text{pilots}} = \{0, L, 2L, \dots, FL\} \quad (55)$$

$$\mathbb{N}_{\text{payload}} = \{1, \dots, N\} \setminus \mathbb{N}_{\text{pilots}}. \quad (56)$$

We also integrated the notation so that the CBC algorithm is naturally the first iteration ($i = 1$) of the EP algorithm, i.e., $z_{\Sigma,n}^{(0)}(a) = z_{g,n}(a)$ and thus $\eta_{\Sigma,n}^{(0)}(a) = \eta_{g,n}(a)$, see (34); the main distinction we need to make is that the smoothing (54) is not applied for $i = 1$, see lines 14–19 of the algorithm. Note that the notation with the iteration index $^{(i)}$ may be removed (and the in-place calculation carried out) but we kept it for compatibility with the equations in the paper.

Last but not least, and at the risk of stating the obvious, we want to emphasize what the EP algorithm is *not* doing. Namely, it is not reusing the output “extrinsic” log-probabilities $\hat{P}_n(a)$ as if they were newly calculated prior log-probabilities $\hat{P}_n^a(a)$. This is clearly seen in the description of the algorithm: plugging $\hat{P}_n(a)$ calculated at line 35 into the line 12 will *not* yield the same results $\eta_{\Sigma,n}^{(i-1)}(a)$.

Since the EP phase tracking is an iterative process itself, the notion of scheduling has to be revised; we use now the notation $\{I_{\text{loop}} \times (I_{\text{ep}}, I_{\text{dec}})\}$ which takes into account the fact that within each loop the phase tracking may execute I_{ep} EP iterations. With this notation, the original CBC algorithm is denoted as $I_{\text{dec}} \times (1, 1)$ and one-shot EP phase tracking is identified by the scheduling $1 \times (I_{\text{ep}}, I_{\text{dec}})$

D. Numerical results

Considering the transmission scenario from Sec. IV-E we evaluate the PER in the one-shot phase tracking (the scheduling $1 \times (I_{\text{ep}}, I_{\text{dec}})$); as discussed in Sec. IV-E, the performance limit for one-shot phase tracking is the DMP (with I_{dec} decoding operations).

The results are shown in Fig. 3 and we observe the following:

- The one-shot EP phase tracking with the scheduling $\{1 \times (2, 10)\}$ outperforms the CBC algorithm (scheduling, $\{30 \times 1\}$) notably, despite the fact that the later requires 20 more decoding iterations and 28 more MPs (and, of course, 28 more projections (34)). The same comparison can be made with the CBC (scheduling $\{10 \times 1\}$): although the complexity measured by the number of decoding iteration is the same, the number of MPs is still larger in the CBC algorithm. Using the EP we thus gain, both in terms of complexity and performance. Moreover, the EP phase tracking operates independently of the decoder which is a significant advantage.
- Increasing the number of EP iterations from $I_{\text{ep}} = 2$ to $I_{\text{ep}} = 3$ improves the performance in low SNR at the cost of the PER saturating in high SNR. However, the choice of the operating

Algorithm 1 EP phase tracking

1: **Inputs:**

2: $y_n, n \in \{0, \dots, N\}$ ▷ Received signal
 3: $x_n, n \in \mathbb{N}_{\text{pilots}}$ ▷ Pilot symbols
 4: $\hat{P}_n^a(a)$ ▷ Log-probabilities from the decoder

5: **Initialization:**

6: $z_{\tilde{\gamma},n}^{(i)} \leftarrow 2^{\frac{y_n x_n^*}{N_0}}, n \in \mathbb{N}_{\text{pilots}}, i \in 1, \dots, I_{\text{ep}}$
 7: $z_{g,n}(a) \leftarrow 2^{\frac{y_n a^*}{N_0}}, a \in \mathcal{A}, n \in \mathbb{N}_{\text{payload}}$
 8: $z_{\Sigma,n}^{(0)}(a) \leftarrow z_{g,n}(a), n \in \mathbb{N}_{\text{payload}}$

9: **EP iterations:**

10: **for** $i \leftarrow 1, \dots, I_{\text{ep}}$ **do** ▷ Finds $\tilde{\gamma}_n(\theta)$:

11: **for** $n \leftarrow \mathbb{N}_{\text{payload}}$ **do**
 12: $\eta_{\Sigma,n}^{(i-1)}(a) \leftarrow -\frac{|a|^2}{N_0} + \hat{I}_0(|z_{\Sigma,n}^{(i-1)}(a)|) + \hat{P}_n^a(a)$
 13: $z_{\text{post},n}^{(i)} \leftarrow \text{CMM}\left[\eta_{\Sigma,n}^{(i-1)}(a), z_{\Sigma,n}^{(i-1)}(a) \mid a \in \mathcal{A}\right]$
 14: **if** $i = 1$ **then**
 15: $z_{\tilde{\gamma},n}^{(i)} \leftarrow z_{\text{post},n}^{(i)} - z_{\alpha,n}^{(i-1)} - z_{\beta,n}^{(i-1)}$
 16: **else**
 17: $z_{\tilde{\gamma},n}^{(i)} \leftarrow \zeta \left(z_{\text{post},n}^{(i)} - z_{\alpha,n}^{(i-1)} - z_{\beta,n}^{(i-1)} \right) + (1 - \zeta) z_{\tilde{\gamma},n}^{(i-1)}$
 18: **end if**
 19: **end for**
 20: $z_{\alpha,0}^{(i)} \leftarrow 0$
 21: **for** $n \leftarrow 1, \dots, N$ **do** ▷ Finds $\alpha_n^{(i)}(\theta)$:
 22: $z_{\alpha,n}^{(i)} \leftarrow \frac{z_{\alpha,n-1}^{(i)} + z_{\tilde{\gamma},n-1}^{(i)}}{1 + |z_{\alpha,n-1}^{(i)} + z_{\tilde{\gamma},n-1}^{(i)}| \sigma_w^2}$
 23: **end for**
 24: $z_{\beta,N}^{(i)} \leftarrow 0$
 25: **for** $n \leftarrow N - 1, \dots, 0$ **do** ▷ Finds $\beta_n^{(i)}(\theta)$:
 26: $z_{\beta,n}^{(i)} \leftarrow \frac{z_{\beta,n+1}^{(i)} + z_{\tilde{\gamma},n+1}^{(i)}}{1 + |z_{\beta,n+1}^{(i)} + z_{\tilde{\gamma},n+1}^{(i)}| \sigma_w^2}$
 27: **end for**
 28: **for** $n \leftarrow \mathbb{N}_{\text{payload}}$ **do**
 29: $z_{\Sigma,n}^{(i)} \leftarrow z_{g,n}(a) + z_{\alpha,n}^{(i)} + z_{\beta,n}^{(i)}$
 30: **end for**
 31: **end for**
 32: **end for**

33: Output: log-probabilities to be used in (9)

34: **for** $n \leftarrow \mathbb{N}_{\text{payload}}$ **do** ▷ Finds $\hat{P}_n(a)$:

35: $\hat{P}_n(a) \leftarrow -\frac{|a|^2}{N_0} + \hat{I}_0(|z_{\Sigma,n}^{(I_{\text{ep}})}(a)|)$
 36: **end for**

point may be different between applications so the “optimal” choice of the parameters is an open issue.

- Some gain is further obtained by increasing the number of operations from $I_{\text{dec}} = 10$ to $I_{\text{dec}} = 30$, yet the qualitative behaviour remains the same.

Despite a notable improvement in terms of complexity and performance when comparing to the CBC algorithm, we still observe the saturation of the PER for high SNR.

While this may be an acceptable solution at least in a context where only one-shot phase tracking is allowed, putting the EP phase-tracking in the decoding loop, changes the picture even more notably as shown in Fig. 4. Since we consider the scheduling $3 \times (I_{\text{ep}}, 10)$, the reference curves are those obtained with $I_{\text{dec}}^{\Sigma} = 30$ decoding iterations. We observe that

- The saturation of the PER disappears thanks to the feedback from the decoder which, already after the first EP phase-tracking and $I_{\text{dec}} = 10$ decoding iterations provides a reliable prior $\hat{P}_n^a(a)$.
- The EP results are better than those yield by the DMP (with $I_{\text{dec}} = 30$); this is quite an impressive results as we are not aware of the results in the literature which would show such a performance; and while it might be surprising at the first sight, it is also correct: remember, the performance limit for the joint decoding-phase tracking is defined by the “All-pilots” curve ($I_{\text{dec}} = 30$).
- As for the complexity, the EP phase tracking with a scheduling $\{3 \times (I_{\text{ep}}, 10)\}$ requires the same number of decoding iterations as the CBC algorithm ($I_{\text{dec}} = 30$). The result of the latter appear only for high SNR and thus, due to the change in the SNR axis range, they are not plotted in Fig. 4. Still, the number of the MP is much lower in the case of the proposed EP algorithm so again, we not only gained notably in performance comparing to the CBC algorithm but also preserved the lower complexity.

VI. CONCLUSIONS

This work was concerned with developing of an algorithm for the phase tracking in single-carrier transmission. This problem often was solved in the literature via message passing (MP) on the graph which describes the relationship between all involved random variables; the performance of the discretized message passing (DMP) was considered a reference.

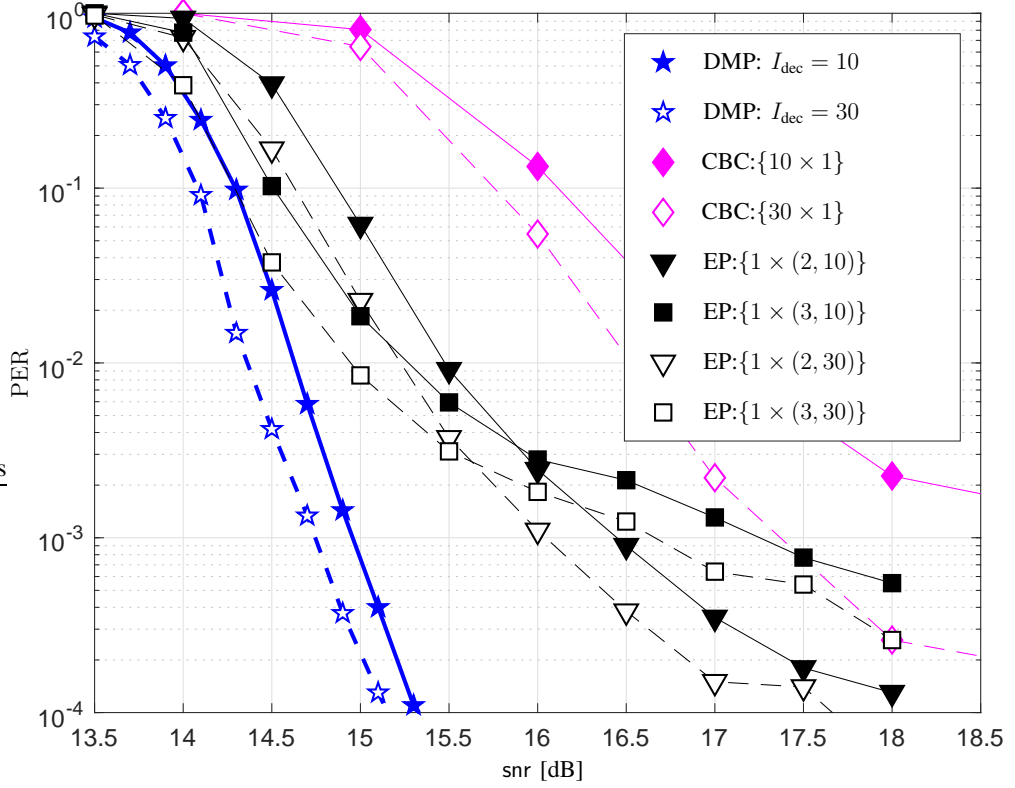


Fig. 3. PER vs. SNR obtained using the EP one-shot phase tracking, that is, the scheduling $\{1 \times (I_{\text{ep}}, I_{\text{dec}})\}$, and the CBC algorithm (scheduling $\{I_{\text{dec}} \times 1\}$). The DMP results are obtained with $I_{\text{dec}} = 10$ (filled markers, solid lines) and $I_{\text{dec}} = 30$ (hollow markers, dashed lines).

We first recognized that the algorithms from the literature, inspired mostly by the Colavolpe–Barbieri–Caire algorithm [1] relied heavily on the feedback from the decoder. As noted already in [6], this approach results in undesirable error floor, especially for large coding rates. We modified the CBC algorithm exploiting the circularity of the involved distributions which notably improved the algorithm.

We further focused on the signal processing approach to the phase-tracking that does not require feedback from the decoder and proposed to improve the solution in an iterative manner. Applying the expectation propagation (EP) we obtained an algorithm which outperforms the known solution even before any feedback from the decoder is available. Further, reusing the decoder’s feedback we attained the performance which is better than the reference of the DMP – the results which, up to our best knowledge, were not yet presented in the literature.

Moreover, comparing to the solutions known from the literature, the proposed EP phase

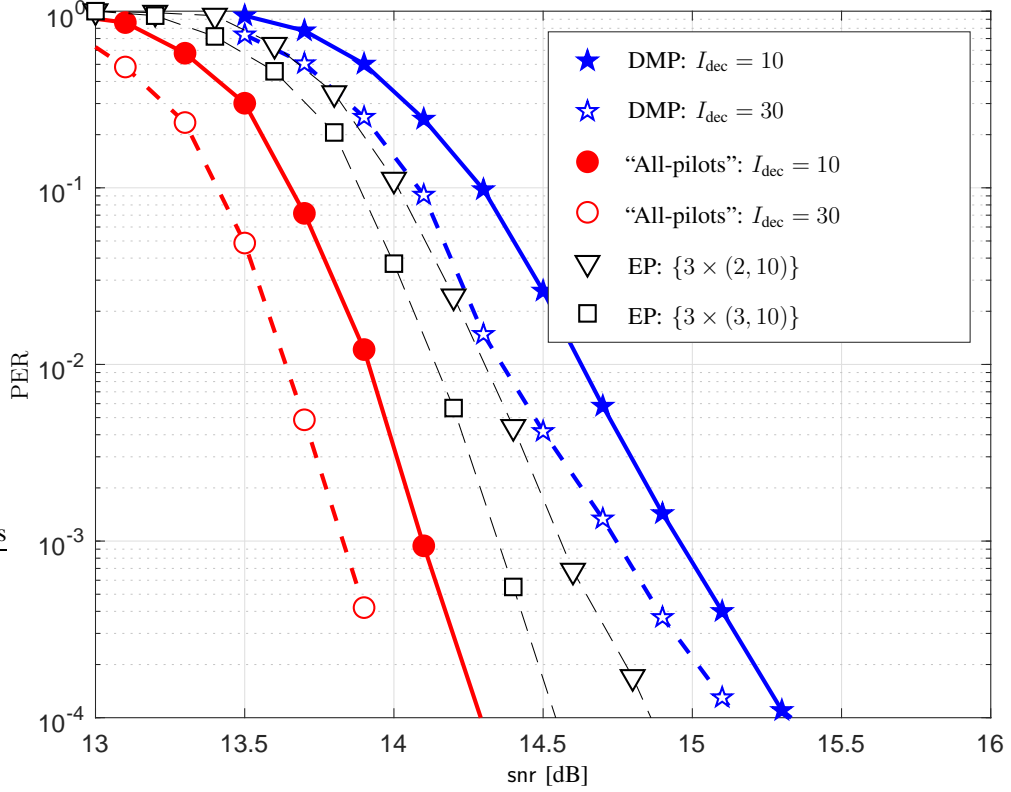


Fig. 4. PER vs. SNR obtained using the EP algorithm in the joint decoding-phase tracking algorithm, with the scheduling $\{3 \times (I_{\text{ep}}, 10)\}$. The DMP and “All-pilots” results are obtained with $I_{\text{dec}} = 10$ (filled markers, solid lines) and $I_{\text{dec}} = 30$ (hollow markers, dashed lines)

tracking not only offers better performance but its computations complexity is lower.

APPENDIX

A. Circular moment matching

The first circular moment of the circular distribution $g(\theta)$ is defined as

$$\mu = \mathbb{M}[g(\theta)] = \int_0^{2\pi} g(\theta) e^{j\theta} d\theta \quad (57)$$

and its angle, $\angle\mu$ defines the circular mean of the underlying variable while its absolute value $|\mu|$ is a measure of concentration (or, precision) which may be thought of the inverse of the variance. In particular,

$$\mathbb{M}[\mathcal{T}(\theta; z)] = B(|z|) e^{j\angle z}, \quad (58)$$

where

$$B(x) = \frac{I_1(x)}{I_0(x)} \quad (59)$$

and $I_1(x)$ is the first-order Bessel function. Since $B(x)$ is not available in closed-form, we propose a simple approximation in Appendix B.

The CMM consists in finding a Tikhonov distribution $\tilde{g}(\theta) = \mathcal{T}(\theta; z_{\tilde{g}})$ closest in the sense of the KL distance to a distribution $g(\theta)$ and amounts to solving the optimization problem

$$z_{\tilde{g}} = \operatorname{argmin}_z \int_0^{2\pi} g(\theta) \log \frac{g(\theta)}{\tilde{g}(\theta; z)} d\theta \quad (60)$$

$$= \operatorname{argmax}_z \int_0^{2\pi} g(\theta) \Re[z e^{-j\theta}] d\theta - \log I_0(|z|) \quad (61)$$

$$= B^{-1}(|\mu|) e^{j\angle\mu}, \quad (62)$$

where $B^{-1}(\cdot)$ is the inverse of $B(x)$; the approximation is given in Appendix B.

For the Tikhonov mixture we deal with in (34), $g(\theta) = \sum_{m=0}^{M-1} \xi_m \mathcal{T}(\theta; z_m)$, we ensure first the normalization. $\sum_{m=0}^{M-1} \xi_m = 1$, and using (58) we calculate the circular moment of the mixture

$$\mu = \mathbb{M}[g(\theta)] = \sum_{m=0}^{M-1} \xi_m B(|z_m|) e^{j\angle z_m}. \quad (63)$$

Then, from (62) we obtain immediately

$$\mathcal{T}(\theta; z_{\tilde{g}}) = \mathcal{F} \left[\sum_{m=0}^{M-1} \xi_m \mathcal{T}(\theta; z_m) \right] \quad (64)$$

$$\angle z_g = \angle \left(\sum_{m=0}^{M-1} \xi_m B(|z_m|) e^{j\angle z_m} \right), \quad (65)$$

$$|z_g| = B^{-1}(|\mu|) = B^{-1}(\mu e^{-j\angle\mu}) \quad (66)$$

$$= B^{-1} \left(\sum_{m=0}^{M-1} \xi_m B(|z_m|) \cos(\angle z_m - \angle z_g) \right). \quad (67)$$

Applying in (64) and (67) the large-argument approximations of $B(|z|)$ given in (68) we obtain the results shown in [5, Eq. (100) and Eq. (101)].

B. Approximation of the function $B(x) = \frac{I_1(x)}{I_0(x)}$

We approximate $B(x)$ and its inverse as

$$B(x) \approx \begin{cases} \frac{1}{2}x & \text{if } x \leq 1 \\ 1 - \frac{1}{2x} & \text{if } x > 1 \end{cases}, \quad (68)$$

$$B^{-1}(y) \approx \begin{cases} 2x & \text{if } y \leq \frac{1}{2} \\ \frac{1}{2(1-y)} & \text{if } y > \frac{1}{2} \end{cases} \quad (69)$$

The large-argument approximation in (68) (case $x > 1$) is known, e.g., [5, Appendix A] but becomes negative for $x < 0.5$. While most often x is assumed large, e.g., $x > 2$ [5, Appendix A] – in which case the large-argument approximation is quite precise, see Fig. 5, it is not uncommon to obtain distributions with $x = \approx 0$. In such a case the large-argument approximation leads to approximation errors which are quite pernicious: even if approximating $B(x)$ with a negative number $B(x) \approx 1 - \frac{1}{2x}$ makes no sense, such an error is difficult to spot as it may appear in the sum of complex numbers: see, for example (63) in the moment-matching procedure described in Appendix A.

In our simulation, such errors were relatively rare and did not lead to significant differences in performance, nevertheless, we believe it is much more sound to use the approximation which covers the entire range of the admissible arguments. This issue motivates us to introduce the small-argument approximation (for $x \leq 1$) which is obtained via Taylor series development of $B(x)$ around $x = 0$. Both, the large-, and the small-argument approximations meet at $x = 1$ which is the threshold for using one approximation or another in (68). The approximation (69) is obtained inverting (68).

We show in Fig. 5 the function $B(x)$ and its approximation (68). The discrepancies between the function are tolerable but more importantly, unlike the previously used large-argument approximation, which was meaningful only for $x > \frac{1}{2}$, we cover all range of the argument x using simple to implement functions. Of course, if necessary, the function $B(x)$ may be also implemented via lookup table.

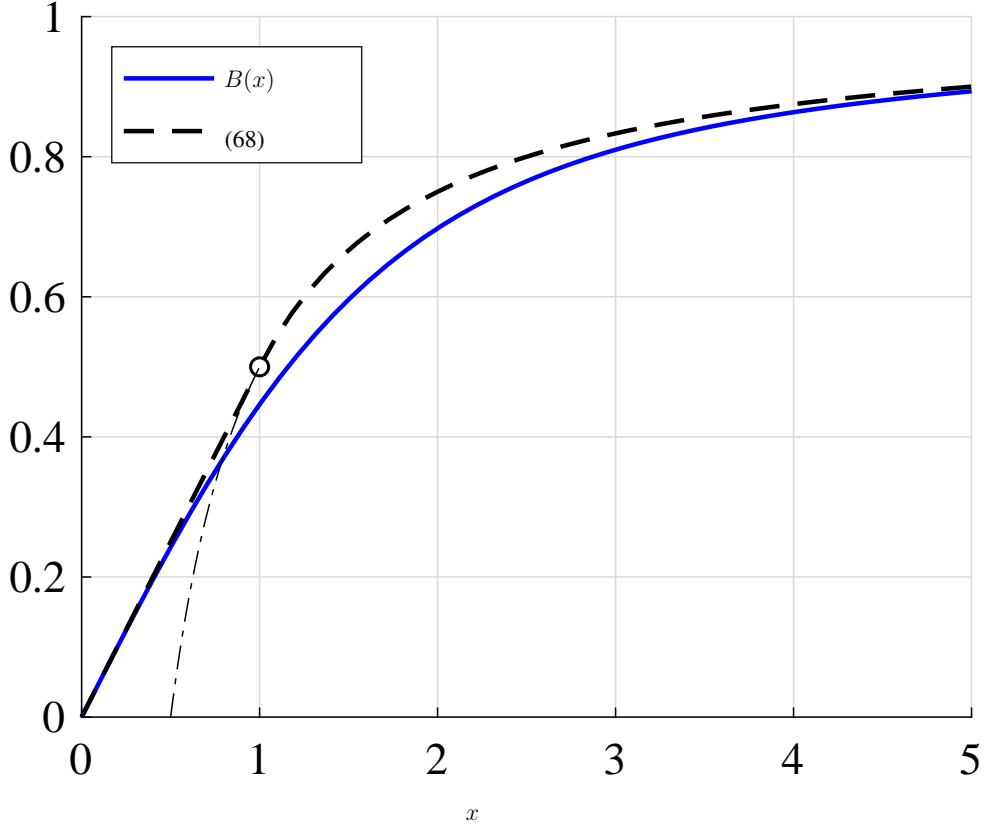


Fig. 5. Comparison between $B(x)$ (solid) and its two-interval approximation from (68) (dashed). The interval limit at which the two approximations merge is shown with a circle. The approximation based on the large-argument value is shown as well (dashed-dotted) but only for $x \geq \frac{1}{2}$ as the function becomes negative for $x < \frac{1}{2}$.

C. Convolving Tikhonov and Gaussian distributions

The convolution of the Tikhonov and the Gaussian distributions may be obtained by moment matching principle [10, Lemma 3]: the result of the convolution should have the same moment as the product of the moments of the convolved distributions.

The first moment of a Gaussian distribution $\mathcal{N}(\theta; 0, \sigma^2)$ is given by $e^{-\frac{\sigma^2}{2}} \approx (1 - \frac{\sigma^2}{2})$, where the approximation is valid for small σ^2 . We can then write

$$\mathcal{T}(\theta; z) * \mathcal{N}(\theta; 0, \sigma^2) \approx \mathcal{T}(\theta; C(z, \sigma^2)) \quad (70)$$

$$C(z, \sigma^2) \approx B^{-1} \left(B(|z|) \left(1 - \frac{\sigma^2}{2} \right) \right) e^{j\angle z}. \quad (71)$$

For $|z| > 1$, using in (71) the large-argument approximation of $B(x)$, shown in (68), yields

$$B(|z|)\left(1 - \frac{\sigma^2}{2}\right) \approx \left(1 - \frac{1}{2|z|}\right)\left(1 - \frac{\sigma^2}{2}\right) \approx 1 - \frac{1}{2|z|} - \frac{\sigma^2}{2}, \quad (72)$$

and, for $|z| < 1$, the small-argument approximation of $B(x)$ allows us to write (71) as

$$C(z, \sigma^2) = \begin{cases} \frac{z}{|z|\sigma^2+1} & \text{if } |z| > 1 \\ z\left(1 - \frac{\sigma^2}{2}\right) & \text{if } |z| \leq 1. \end{cases} \quad (73)$$

We note that the large-argument case ($|z| > 1$) was already used previously, e.g., in [1] [11] [5]. Both approximations yield quite similar results and using the large-argument approximation did not affect the results in our simulations.

REFERENCES

- [1] G. Colavolpe, A. Barbieri, and G. Caire, “Algorithms for iterative decoding in the presence of strong phase noise,” *IEEE J. Sel. Areas Commun.*, vol. 23, no. 9, pp. 1748–1757, Sep. 2005.
- [2] H. ShahMohammadian and A. Aharony, “Accurate BCJR-based synchronization algorithm for single carrier channels with extremely high order modulations,” in *2016 10th International Conference on Signal Processing and Communication Systems (ICSPCS)*, 2016, pp. 1–6.
- [3] D. S. Millar, R. Maher, D. Lavery, T. Koike-Akino, M. Pajovic, A. Alvarado, M. Paskov, K. Kojima, K. Parsons, B. C. Thomsen, S. J. Savory, and P. Bayvel, “Design of a 1 Tb/s superchannel coherent receiver,” *J. Lightw. Technol.*, vol. 34, no. 6, pp. 1453–1463, Mar. 2016.
- [4] A. F. Alfredsson, E. Agrell, and H. Wymeersch, “Iterative detection and phase-noise compensation for coded multichannel optical transmission,” *IEEE Trans. Commun.*, vol. 67, no. 8, pp. 5532–5543, 2019.
- [5] S. Shayovitz and D. Raphaeli, “Message passing algorithms for phase noise tracking using Tikhonov mixtures,” *IEEE Trans. Commun.*, vol. 64, no. 1, pp. 387–401, Jan. 2016.
- [6] A. Kreimer and D. Raphaeli, “Efficient low-complexity phase noise resistant iterative joint phase estimation and decoding algorithm,” *IEEE Trans. Commun.*, vol. 66, no. 9, pp. 4199–4210, Sep. 2018.
- [7] S. Pecorino, S. Mandelli, L. Barletta, M. Magarini, and A. Spalvieri, “Bootstrapping iterative demodulation and decoding without pilot symbols,” *Journal of Lightwave Technology*, vol. 33, no. 17, pp. 3613–3622, 2015.
- [8] T. P. Minka, “A family of algorithms for approximate Bayesian inference,” Ph.D. dissertation, Massachusetts Institute of Technology, 2001.
- [9] L. Szczechinski and A. Alvarado, *Bit-Interlaved Coded Modulation : Fundamentals, Analysis and Design*. Wiley, 2015.
- [10] G. Kurz, I. Gilitschenski, and U. D. Hanebeck, “Recursive Bayesian filtering in circular state spaces,” *IEEE Aerosp. Electron. Syst. Mag.*, vol. 31, no. 3, pp. 70–87, 2016.
- [11] A. Barbieri, G. Colavolpe, and G. Caire, “Joint iterative detection and decoding in the presence of phase noise and frequency offset,” *IEEE Trans. Commun.*, vol. 55, no. 1, pp. 171–179, 2007.
- [12] Y. Xu, L. Szczechinski, B. Rong, F. Labeau, D. He, Y. Wu, and W. Zhang, “Variable LLR scaling in min-sum decoding for irregular LDPC codes,” *IEEE Trans. Broadcast.*, vol. 60, no. 4, pp. 606–613, Dec. 2014.

- [13] M. Senst and G. Ascheid, "How the framework of expectation propagation yields an iterative IC-LMMSE MIMO receiver," in *IEEE Global Comm. Conf. (GLOBECOM)*, Dec. 2011, pp. 1–6.
- [14] J. Céspedes, P. M. Olmos, M. Sánchez-Fernández, and F. Pérez-Cruz, "Expectation propagation detection for high-order high-dimensional MIMO systems," *IEEE Trans. Commun.*, vol. 62, no. 8, pp. 2840–2849, 2014.